ACS APPLIED MATERIALS & INTERFACES

Research Article

www.acsami.org

One-Pot Synthesis of Copper Sulfide Nanowires/Reduced Graphene Oxide Nanocomposites with Excellent Lithium-Storage Properties as Anode Materials for Lithium-Ion Batteries

Caihong Feng,[†,‡] Le Zhang,[†] Menghuan Yang,[†] Xiangyun Song,[‡] Hui Zhao,[‡] Zhe Jia,[‡] Kening Sun,*[,†] and Gao Liu*[,‡]

[†]School of Chemical Engineering and Environment, Beijing Institute of Technology, Beijing, 100081, People's Republic of China

[‡]Lawrence Berkeley National Laboratory, 1 Cyclotron Road, MS 70R108B, Berkeley, California 94720, United States

Supporting Information

ABSTRACT: Copper sulfide nanowires/reduced graphene oxide (CuSNWs/rGO) nanocompsites are successfully synthesized via a facile one-pot and template-free solution method in a dimethyl sulfoxide (DMSO)−ethyl glycol (EG) mixed solvent. It is noteworthy that the precursor plays a crucial role in the formation of the nanocomposites structure. SEM, TEM, XRD, IR and Raman spectroscopy are used to investigate the morphological and structural evolution of CuSNWs/rGO nanocomposites. The as-fabricated CuSNWs/rGO nanocompsites show remarkably improved Li-storage performance, excellent cycling stability as well as high-rate capability compared with pristine CuS nanowires. It obtains a reversible capacity of 620 mAh g^{-1} at 0.5C (1C = 560 mA g^{-1}) after 100 cycles and 320 mAh g^{-1} at a high current rate of 4C even after 430 cycles. The excellent lithium storage performance is ascribed to the synergistic effect between CuS nanowires and rGO nanosheets. The as-formed CuSNWs/rGO nanocomposites can effectively accommodate large volume changes, supply a 2D conducting network and trap the polysulfides generated during the conversion reaction of CuS.

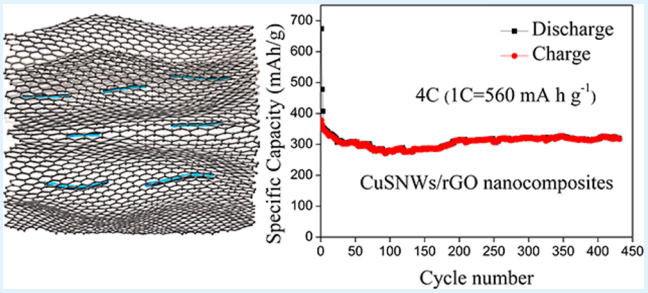

KEYWORDS: *copper sulfide, reduced oxide graphene, nanocomposites, lithium-ion battery, synergistic effect*

1. INTRODUCTION

The increasingly emerging energy and environmental issues have constantly inspired enormous amount of research interest in advanced energy conversion and storage (ECS) devices.[1−3] The performance of these devices depends intimately on the properties of their materials, so it is critical to find innovative materials with new properties or modification routine ECS materials to meet the improving requirement for clean, efficient and sustainable energy supply.[4,5] Metal chalcogenides (MCs) are attracting significant attention due to their various applications in ECS devices including photocatalytic material, photothermal material, solar cells, electrocatalysis, Li-ion batteries (LIBs) and supercapacitors.[6−10] The successful utilization of ECS devices depends critically on the synthesis of new nanostructured materials of different sizes and new morphologies,[1,2,4−6] but it is still a challenge to find a simple and easy way to large preparation nanostructured materials with designed structure and morphologies.

Copper sulfides (Cu_xS) including CuS, $Cu_{1.96}S$, $Cu_{1.8}S$ and Cu_2S are useful materials for energy storage applications due to their cost effectiveness and abundance in nature.[11−13] CuS has been used as electrode materials in LIBs owing to its good electrical conductivity (10^{-3} S cm^{-1}), high theoretical capacity (560 mAh g^{-1}) and flat discharge curves.[14,15] However, like most metal sulfide, it has some major drawbacks, namely capacity fading and poor cyclability, which are associated with the pulverization of electrodes resulting in the decay of the specific capacity and formation of polysulfides Li_2S_x ($2 < x < 8$).[14,16,17] The polysulfides, intermediates of the electrochemical reactions, can easily dissolve into organic electrolyte and migrate to the anode side leading to the poor capacity retention of LIBs. To deal with these issues, CuS micro/nanostructures with different morphologies have been extensively investigated to improve their electrochemical properties by creating short diffusion lengths for Li^+ ions and increasing flexibility toward volume caused by Li^+ insertion/extraction. For example, Cai et al.[12] have synthesized Cu_xS/Cu nanotubes and found that the nanotubes electrode present high discharge capacity of 526 mAh g^{-1} at a current density of 200 mA g^{-1} and good rate capability (282 mAh g^{-1} at 5 A g^{-1}). Zhang's group[18] synthesized ultrathin CuS nanosheets that exhibit a large capacity, good cycling stability, and the capacity sustains at 642 mAh g^{-1} after 360 cycles at a current rate of 0.2 A g^{-1}. In addition, many researchers have to limit the potential window

Received: February 9, 2015
Accepted: July 2, 2015
Published: July 2, 2015

DOI: 10.1021/acsami.5b01285
ACS Appl. Mater. Interfaces 2015, 7, 15726−15734

by sacrificing capacity to avoid lithium polysulfides dissolution.[14,19,20]

The ability to modify chemically an electrode nanomaterial with carbon-based materials, especially activated carbon, carbon nanotubes (CNTs) and graphene, offers an intriguing route to engineer target materials with multifunctionalities or improved properties because of its high conductivities and large surface areas.[4] For example, SiNW-G composite, CNT−graphene−Si composites and TiO_2/graphene have been reported to exhibit excellent electrochemical performance as the anode for LIBs.[21−24] Recently, studies showed that capping the sulfur or metal sulfide with thin graphene or graphene oxide layer could effectively reduce the dissolution of Li_2S_x into the electrolyte, and led to high reversible capacities and good rate capabilities.[25−27] This could be a promising strategy for the copper sulfide used as high performance electrode in LIBs by wrapping CuS nanocraystals with graphene to get high electrical conductivity, effective accommodation of the strain during Li^+ insertion/extraction and reduce polysulfide dissolution into the electrolyte during the repeated charging and discharging as well. Very recently, Tao et al.[28] reported synthesis of a CuS/graphene composite as an anode material for LIBs and the obtained CuS/graphene composite exhibits a relative high reversible capacity and good cycling stability. Ren and co-workers also reported a double-sandwiched-like CuS/rGO structure for LIBs anode materials with enhanced electrochemical properties.[29] But there still exist challenges to meet the demanding requirements for LIBs with high charging/discharging rate, high capacity and long cycle life. One-dimensional CuS nanowires have attracted wide interest as the electrode for LIBs due to their advantages in electronic conduction along the axial direction.[15,19] Encouraged by this, design and fabricate CuS nanowires/graphene composites could be a promising solution for high-performance LIBs electrode material. Though different shapes of CuS and CuS/graphene as electrode materials for LIBs have been studied, there are few reports about CuS nanowires. It is difficult to find a simple method for the large-scale synthesis of a CuS nanowires/graphene composite. To the best of our knowledge, there is no report on the synthesis and electrochemical properties of it.

Herein, we develop a facile, one-pot approach to prepare CuSNWs/rGO nanocomposites by mixed solvent of dimethyl sulfoxide (DMSO) and ethylene glycol (EG). Compared with other methods,[29−32] we successfully gained the nanocomposites without any surfactants and additional reductant. The rGO nanosheets act as a conductive, elastically strong and electrochemically active substrate to produce the CuSNWs/rGO nanocomposites as anode materials. More importantly, this nanocomposites could relieve the polysulfides dissolution. With the synergistic effect of CuS nanowires and rGO nanosheets, the as-produced CuSNWs/rGO nanocomposites are promising for application as high-rate LIBs electrode materials.

2. EXPERIMENTAL SECTION

2.1. Materials. Thiourea (AR, 99.0%), copper(II) nitrate trihydrate ($Cu(NO_3)_2·3H_2O$, AR, 99.5%), ethylene glycol (EG, AR) and dimethyl sulfoxide (DMSO, AR) were purchased from Beijing Chemical Company. Lithium-ion electrolytes were purchased from Zhangjiagang Guotai-Huarong New Chemical Materials Co., including 1 M $LiPF_6$ in ethylene carbonate (EC), diethyl carbonate (DEC) and dimethyl carbonate (DMC) with a volume ratio of 1:1:1. All chemicals were used without further purification.

2.2. Synthesis of the CuSNWs/rGO Nanocomposites. Graphene oxide (GO) was prepared from natural graphite powder via a modified Hummers method.[33] In a typical process, 46 mg of GO was dispersed in 90 mL of ethylene glycol (EG) by ultrasonic treatment for 2 h and then centrifuged at 4000 rpm for 20 min to remove undissolved large particles. The suspension was added to a three-necked flask with 30 mL of DMSO and 0.484 g of $Cu(NO_3)_2·3H_2O$ (2 mmol) under magnetic stirring. Then, the flask was placed into oil bath and heated at 145 °C for 6 h under nitrogen atmosphere. Finally, 10 mL of mixed solution containing 0.456 g (6 mmol) of thiourea was added to the solution drop by drop through a syringe under vigorous stirring and reacted for another 1.5 h. The final products were centrifuged and washed several times by distilled water and ethanol, and finally freeze-dried for 48 h for further characterization.

For comparison, pristine CuS nanowires were prepared by a similar process in the absence of graphene oxide as previously reported by our group[15] and bare rGO was synthesized in the same process except without the addition of $Cu(NO_3)_2·3H_2O$.

2.3. Material Characterization. The phase composition of the as-prepared samples were characterized by a Philips X'Pert Pro Multipurpose X-ray diffractometer (XRD) using Cu Kα radiation at 45 kV and 40 mA, at the 2θ range of 5−80° with 0.02 per step. The Raman spectra of the sample were collected using a Renishaw spectrophotometer equipped with a microscope having a laser wavelength of 532 nm. The morphology of the samples and electrodes was characterized with a Quanta FEG 250 (FEI) field emission scanning electronmicroscopy (SEM) system. High-resolution transmission electron microscopy (HRTEM) images were obtained on a JEOL JEM-2100F field emission microscope operated at 200 kV. X-ray photoelectron spectroscopy (XPS) was carried out on a Physical Electronics 5400 ESCA. Fourier transform infrared (FT-IR) spectroscopy analysis was carried out in the range of 400−4000 cm^{-1} using a Nicolet iS10 (Thermo Scientific) spectrometer. TG/DTA analysis were performed with a TG/DTA 6200 (Seiko) apparatus at a heating rate of 10 °C min^{-1} in a flowing air to determine the amount of rGO in the samples.

2.4. Electrochemical Measurement. The coin-type cell were assembled in an argon-filled glovebox, where both moisture and oxygen level were less than 5 ppm. The working electrode was composed of 75 wt % active material (CuSNWs/rGO nanocomposites), 10 wt % acetylene black (super p), 12 wt % CMC and 3 wt % PVA dissolved in water. Lithium foil was used as the counter and reference electrodes, and polypropylene membrane (Celgard 2400) as a separator. The electrolyte solution was 1 M $LiPF_6$ dissolved in a mixture of ethylene carbonate (EC)/diethyl carbonate (DEC)/dimethyl carbonate (DMC) (1:1:1 in volume). The galvanostatic charge/discharge measurements were performed using a Land Battery Measurement System (Wuhan, China) at various current densities of 0.1C−5C (1C = 560 mAh g^{-1}) with a voltage window of 0.02−3.00 V vs Li/Li^+. The cyclic voltammetry (CV) curves of materials were carried out by using CHI660D (Shanghai Chenhua Instrument) at a scanning rate of 0.1 mV s^{-1} between 0.02 and 3.00 V and electrochemical impedance spectroscopy (EIS) in the range of 10 mHz to 100 kHz on PARSTAT 2273. All the performances were tested at room temperature.

3. RESULTS AND DISCUSSION

3.1. Characterizations of Morphology and Structure. The XRD patterns of CuS nanowires, CuSNWs/rGO and GO are shown in Figure 1. All the diffraction peaks in Figure 1a can be indexed to the hexagonal phase of CuS (JCPDS No. 06-0464) and no impurity phases can be detected, indicating the formation of pure CuS and that they are highly crystallized. As shown in Figure 1b, the as-prepared GO after chemical oxidation exhibits a strong and sharp peak at 11.6°, which corresponds to the (002) interplanar spacing of 0.82 nm, indicating that the original sp^2-bond carbon of graphite suffers

DOI: 10.1021/acsami.5b01285
ACS Appl. Mater. Interfaces 2015, 7, 15726−15734

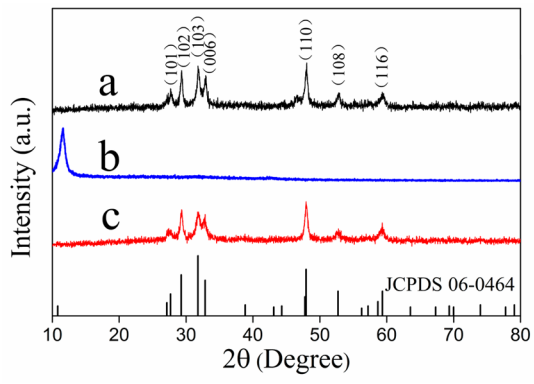

Figure 1. XRD patterns of (a) CuS nanowires, (b) GO and (c) CuSNWs/rGO nanocomposites.

breaking by oxidization.[30] For the CuSNWs/rGO composites (Figure 1c), the characteristic peak of GO disappears due to the considerable reduction capability of EG, DMSO and thiourea at high temperature.[28,32,34] However, the characteristic stacking peak of rGO nanosheets at around 26° cannot be identified from the XRD pattern of CuSNWs/rGO nanocomposites due to its low amount and low diffraction intensity.[28] From the TG analysis of CuSNWs/rGO nanocomposites (Supporting Information, Figure S1), the content of CuS in the composites is about 82.40 wt %. Besides, the broad diffraction peaks of CuS in CuSNWs/rGO composite indicated that the products have small sizes.[25]

The reduction of the GO was also confirmed by Raman spectra. As shown in Figure 2a, both spectra exhibit two characteristic main peaks: the D band at ~1357 cm^{-1} attributes to defects and disorder in the hexagonal graphitic layers and the G band at ~1575 cm^{-1} corresponds to the vibration of sp^2 carbon atoms in a 2D hexagonal lattice.[30−32] It is found that the ration value of I_D/I_G for CuSNWs/rGO nanocomposites and rGO is 1.14 and 1.07, respectively, which is higher than that of GO (0.86). The increased I_D/I_G is attributed to the formation of new and smaller sp^2 domains during the reduction, giving evidence that the GO was successfully reduced to form graphene.[26] Moreover, the strong and sharp band at ~475 cm^{-1} in the spectra of CuSNWs/rGO nanocomposites agrees well with the observation for the covellite structure of CuS with a hexagonal crystal structure by previous work.[29,31,32] The Raman results well agree with the XRD data.

The prepared CuSNWs/rGO composites and pristine GO were further investigated by FT-IR measurement. As shown in Figure 2b, the strong and overlapping band at around 3400 cm^{-1} is assigned to the stretching vibration of structural O—H and adsorbed water molecules.[34] The characteristic peak of the C═O stretching vibration appears at 1740 cm^{-1}.[32] Moreover, peaks at 1380, 1270, and 1050 cm^{-1} are observed in the spectrum of GO, which can be indexed to the stretching vibrations of C—OH, C—O—C and C—O, respectively.[33,34] However, most of these oxygen functional groups derived disappear in the spectrum of the CuSNWs/rGO composites, indicating that GO has been reduced to rGO in our reaction system. The results agree well with the result of XRD and further confirm that CuSNWs/rGO nanocomposites can be obtained by our simple, one-pot method. Besides, the peaks of C—S stretching (1097 cm^{-1}) can be found in the spectrum of the CuSNWs/rGO composites indicating that CuS nanowires are chemically bonded to the rGO,[34] and these chemical bonds are important to the stability and electrochemical performance of the CuSNWs/rGO nanocomposites.[22]

SEM and TEM were used to characterize the morphologies of as-prepared CuSNWs/rGO nanocomposites. As shown in Figure 3a,b, the CuS nanowires have rough surfaces and are wrapped by rGO nanosheets. Compared with pristine CuS nanowires (Supporting Information, Figure S2a,b), the nanowires are evenly distributed and the length become shorter than that of pristine CuS nanowires. It is suggested that rGO nanosheets may restrict CuS growth and aggregation.[35,36] More details of CuSNWs/rGO nanocomposite were further investigated by TEM and HRTEM and shown in Figure 3c,d. From the TEM analysis, we can clearly see that CuS nanowires are coated by rGO film and these nanowires are side-by-side and self-assemble into the nanobundle. The HRTEM image (Figure 3d) of CuSNWs/rGO (enclosed by dash line in Figure 3c) shows two kinds lattice fringes. One is not well-defined with interlayer distance (*d*-spacing) of around 0.38 nm corresponding the *d*-spacing of rGO,[28,37] and the other is ordered with fringe spaces of 0.32 nm, which can be indexed as the (101) planes of hexagonal CuS. All the above structural and morphological characterization confirms that CuSNWs/rGO nanocomposites can be easily achieved with this simple and easily controlled approach.

To understand better the formation process of CuSNWs/rGO nanocomposites, control experiments were performed to understand the influence of thiourea. The intermediate in the absence of thiourea and the product after adding thiourea at the beginning of the reaction were studied. As seen in Figure 4a, in the absence of thiourea, we obtained the intermediate

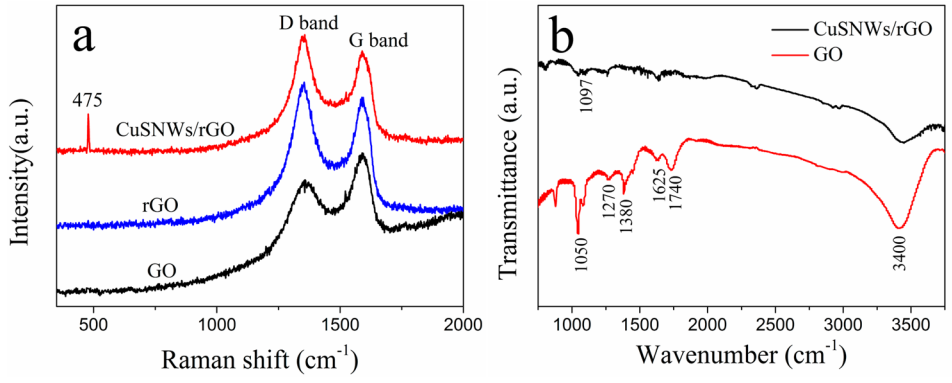

Figure 2. (a) Raman spectra of CuSNWs/rGO nanocomposites, rGO and GO. (b) FT-IR spectra of GO and CuSNWs/rGO nanocomposites.

DOI: 10.1021/acsami.5b01285
ACS Appl. Mater. Interfaces 2015, 7, 15726−15734

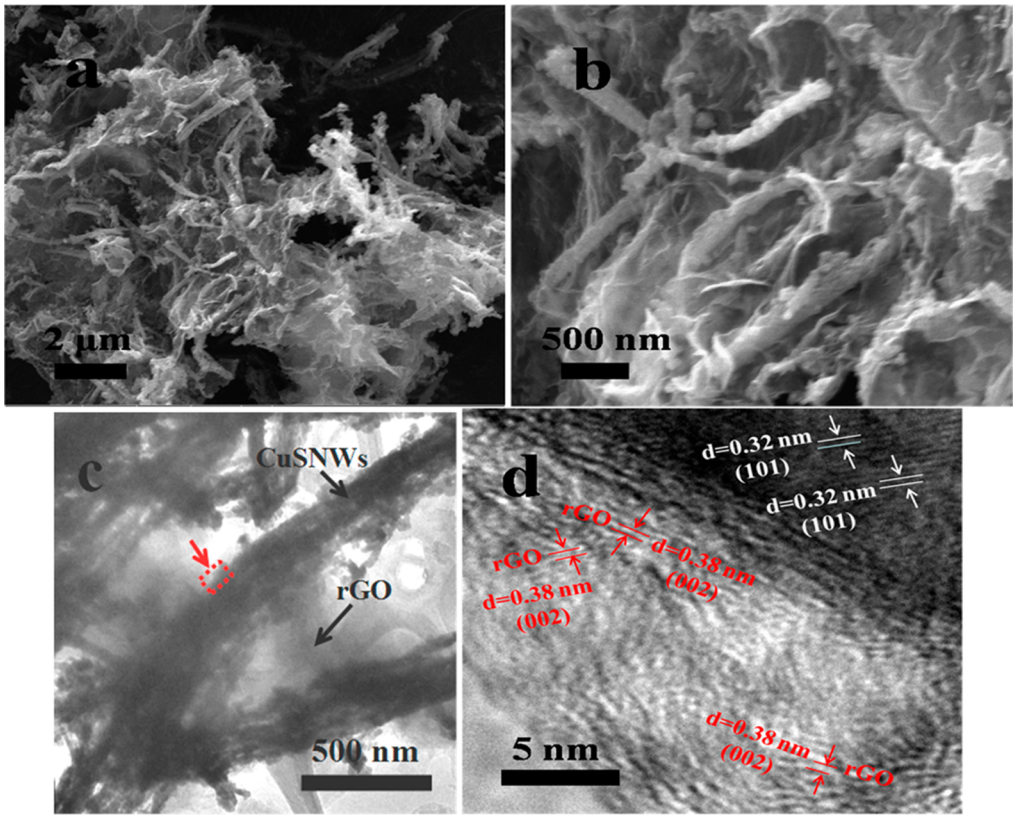

Figure 3. SEM images of CuSNWs/rGO nanocomposites (a) low magnification and (b) high magnification. TEM image of (c) CuSNW/rGO and (d) HRTEM image of CuSNWs/RGO nanocomposites.

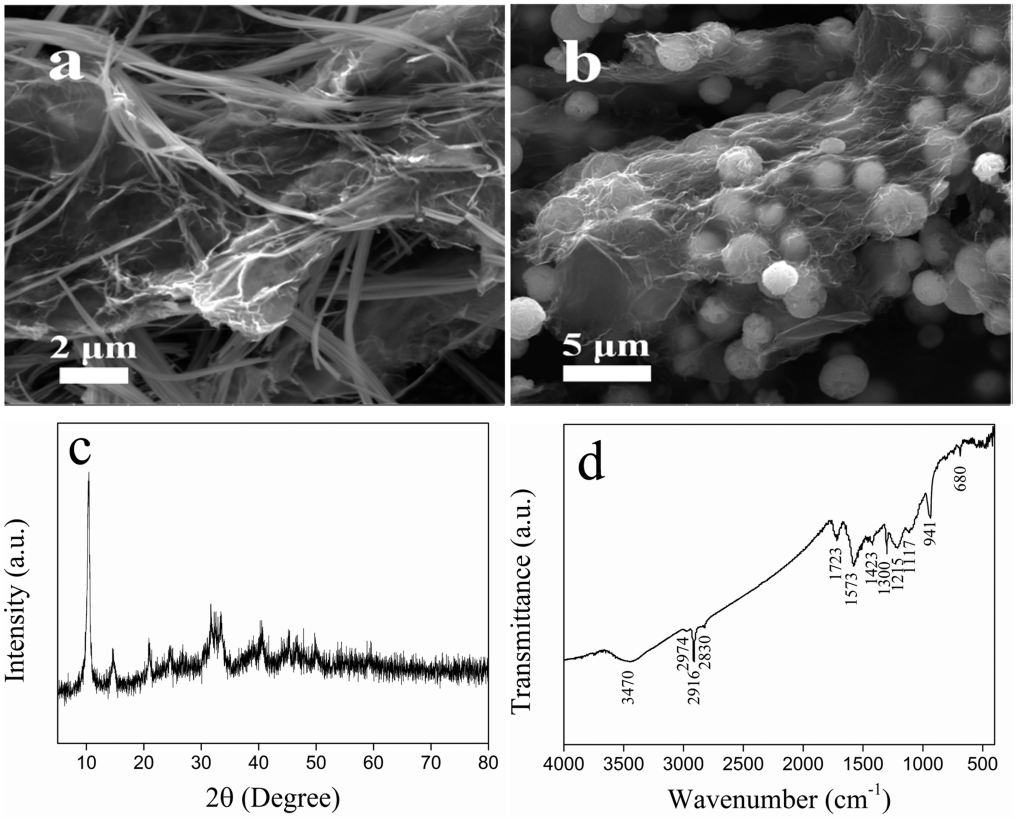

Figure 4. SEM images of (a) intermediate and (b) CuS microshere/rGO composites. (c) XRD pattern of intermediate. (d) FT-IR spectra of intermediate.

DOI: 10.1021/acsami.5b01285
ACS Appl. Mater. Interfaces 2015, 7, 15726−15734

nanowires tens of micrometers long in size with a more smooth surface. When thiourea, $Cu(NO_3)_2{\cdot}3H_2O$ and solvent are added together at the beginning, the morphology of the product is a CuS microsphere instead of nanowires dispersed in the rGO nanosheets (Figure 4b). The XRD pattern of intermediate (Figure 4c) shows a strong peak appearing in the 10.44°, which is striking similarity to those of other metal alkoxide precursors reported in the literature.[38,39] As we all know, DMSO is an excellent solvent. It can interaction with metal anions to form $M(DMSO)^{x+}$ and M−DMSO complexes.[40,41] The peak at 941 cm^{-1} in the FT-IR spectra of intermediate (Figure 4d) corresponds the S═O stretching band in the Cu−DMSO complex.[42] To analyze the chemical composition of intermediate and identify the chemical status of Cu, S, O elements in samples, X-ray photoelectron spectroscopy (XPS) analysis was carried out. The wide-scan XPS spectrum (Supporting Information, Figure S3a) evidently shows the signals of Cu, S, C and O elements. The high-resolution XPS spectra (Supporting Information, Figure S3b−d) analysis shows that the intermediate contains Cu^{2+}, S^{2-} and C—O—R. On the basis of all the results, though we cannot confirm the exact structure of intermediate, we can deduce that the intermediate should a complex of $Cu(DMSO)_n(OCH_2CH_2O)$/rGO and $Cu(DMSO)_nS$/rGO. Besides, the intermediate is vital to the ultimate morphology of the CuS nanowire. It may act as a soft template and convert to final product CuSNWs/rGO nanocomposites after the addition of thiourea. On the basis of the experiment results, the formation process of the CuSNWs/rGO nanocomposites is presented in Scheme 1. First, Cu^{2+} cations favorably bind with

Scheme 1. Illustration of the Formation Process of CuSNWs/rGO Nanocomposites

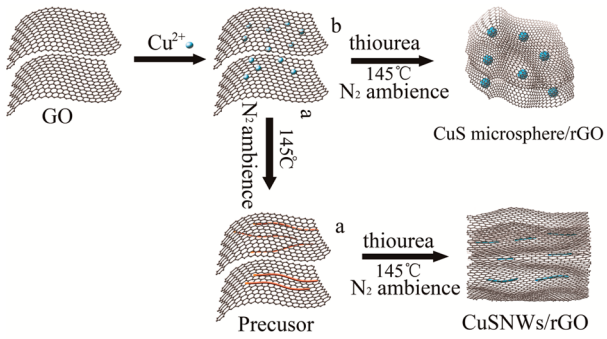

oxygen-containing groups on GO sheets via the electrostatic interactions. If thiourea is added at the beginning, it reacts with Cu^{2+} immediately and only CuS microspheres coated by rGO nanosheets are obtained (Scheme 1b). If thiourea is added after the formation of the precursor, CuS nanowires wrapped by rGO nanocomposites are synthesized, as shown in Scheme 1a. The possible reaction process of CuSNWs/rGO is listed in the Supporting Information, chemical eqs 1−5.

3.2. Electrochemical Performance. The electrochemical properties of the CuSNWs/rGO nanocomposites for reversible Li^+ storage were investigated by eletrochemical measurements. The results are shown in Figure 5.

The cyclic voltammograms of CuSNWs/rGO nanocomposites is given in Figure 5a, which elaborates the oxidation and reduction reactions due to the insertion and extraction of Li^+ into the electrode. In the first cycle, two reduction peaks are observed at around 1.6 and 2.0 V, and two oxidation peaks at around 1.9 and 2.4 V. In the subsequent cycles, one of the main cathodic peaks at 2.0 V shifts toward the higher potential of 2.1 V and similarly the anodic peaks shift slightly negatively. The shift of the main cathodic peak toward a higher potential in the following cycles corresponds to a multistep electrochemical reaction of lithium with the electrode that leads to the formation of a SEI film on the surface of the electrode, decomposition of the electrode and the formation of Li_2S.[25,29] So, the two-step reactions of the the composite are elucidated by the following equations:

$$CuS + xLi^+ + xe^- \leftrightarrow Li_xCuS \quad (1)$$

$$Li_xCuS + (2 - x)Li^+ + (2 - x)e^- \leftrightarrow Li_2S + Cu \quad (2)$$

The transformation from CuS to Li_xCuS is related to the cathodic peak at 2.0 V, whereas that from Li_xCuS to Cu is associated with the cathodic peak at 1.6 V.[14,15,29]

Figure 5b illustrates the charge−discharge voltage profiles of the CuSNWs/rGO nanocomposites electrode for the first, second, tenth and fiftieth cycles at a constant current rate of 0.5C. As shown in Figure 5b, two potential plateaus at around 2.0 and 1.6 V were observed in the initial charge process and two potential plateaus at around 1.9 and 2.4 V in the initial discharge process corresponding to the lithiation and delithiation of CuS electrode were in qualitative agreement with the discharge and charge plateaus in Figure 5a. The plateau at 2.0 V in discharge process and the plateau at 2.4 V in charge process become shorter and shorter. After 10 cycles, only one pair of plateau is observed. Similar results were also observed by Y. Wang's and Y. Ren's work, which implies that the electrochemical reaction change gradually.[14,29] For the CuSNWs/rGO nanocomposites electrode, the potential plateaus of initial charge and charge curves agrees well with that of CuS nanowires electrode (Supporting Information, Figure S4a) except a plateau at around 0.7 V in the first discharge process (Figure 5b). It is well-known that the plateau at about 0.7 V at the initial discharge process for carbon materials is generally ascribed to the formation of SEI film.[43] So, the flat voltage at around 0.7 V should be related to the formation of solid electrolyte interface (SEI) film on the rGO surface. The initial discharge and charge capacities of the CuSNWs/rGO electrode in the first cycle are 908 and 630 mAh g^{-1}, respectively, based on the whole weight of the composite. The large initial discharge capacity of CuSNWs/rGO nanocomposites may be attributed to the SEI layer on the surface of the electrode due to the electrolyte decomposition,[15,28,29] reduction of residual oxygen-containing groups on graphene and the irreversible reaction between Li and CuS as indicated in eqs 1 and 2.[44,45] The decrease in the area of the next cycle is consistent with the charge and discharge curves (Figure 5b), reflecting the capacity fading in subsequent cycles. It should be pointed out that the Coloumbic efficiencies increase to almost unity in the successive cycles, indicating that the formed SEI during the first cycle is favorable and stable.[46]

The cycling performances of CuSNWs/rGO nanocomposites electrode compared with bare CuS nanowires electrode and rGO nanosheets electrode at a current of 0.5 C are shown in Figure 5c (the average capacity and standard deviation of parallel cells is shown Figure S5 in the Supporting Information). It is observed that the initial discharge capacity is 908, 708 and 953 mAh g^{-1} for CuSNWs/rGO nanocomposites, CuS nanowires and rGO nanosheets, respectively.

DOI: 10.1021/acsami.5b01285
ACS Appl. Mater. Interfaces 2015, 7, 15726−15734

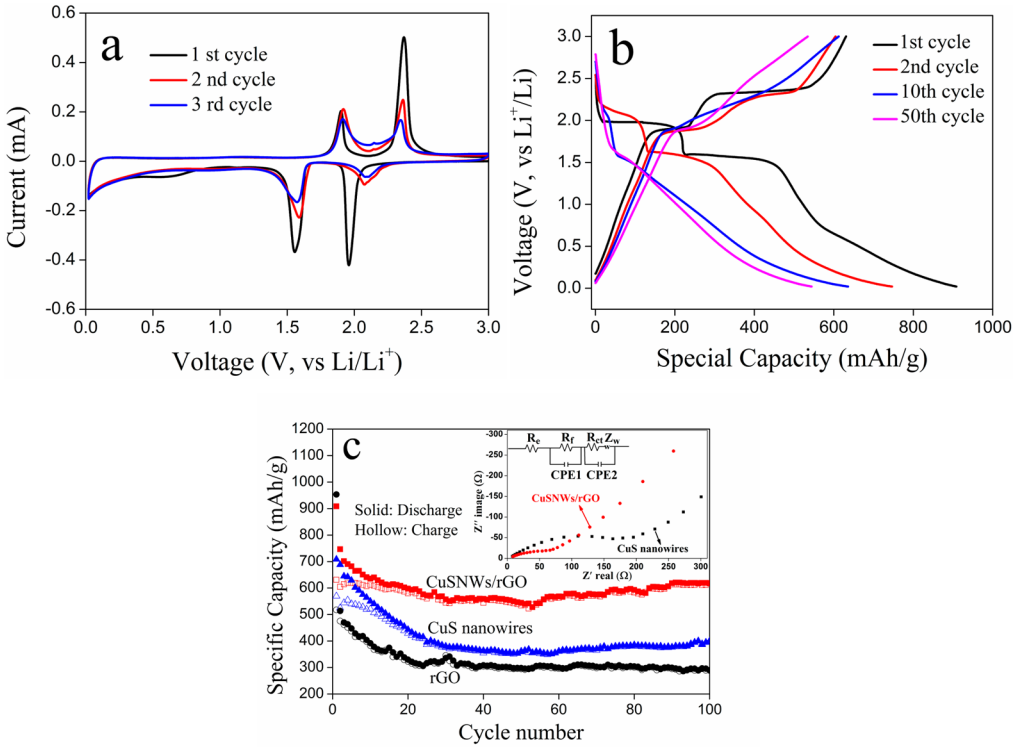

Figure 5. (a) CV response of the CuSNWs/rGO nanocomposites electrode. (b) Charge and discharge curves for the CuSNWs/rGO nanocomposites electrode at a rate of 0.5C between 0.02 and 3.00 V. (c) Cycling performance of the CuSNWs/rGO nanocomposites electrode, CuS nanowires electrode, and rGO electrode at a current density of 0.5C within a voltage window of 0.02−3.00 V. Inset: Nyquist plots of CuSNWs/rGO nanocomposites electrode and CuS nanowires electrode after charge and discharge at 0.5C for 100 cycles and equivalent circuit model of the studied system.

The high initial discharge capacities are attributed to the formation of SEI film. After a few cycles, the CuS electrode shows a significant capacity decrease, whereas the intensity of the capacity decreasing for CuSNWs/rGO is obviously lighter. This may attribute to the introduction of rGO nanosheets, which restricts the diffusion of polysulfides to some extent.[27] The CuS nanowires were wrapped by rGO nanosheets and evenly distributed in them, which can efficiently trap the polysulfides and suppress the outward diffusion of polysulfides. After 100 cycles, the capacity of CuSNWs/rGO maintains at 620 mAh g^{-1}, and for CuS nanowires and rGO electrode the capacity keeps at 400 and 300 mAh g^{-1}, respectively. It is obvious that the composites have a higher capacity than each individual component. Various CuS and CuS/graphene composites as electrode materials for LIBs have been studied; for example, Ma's group has prepared a hybrid network CuS monolith cathode with a capacity of 468.3 mAh g^{-1} after 100 cycles (0.2 C, 1.0−3.0 V).[47] Wang et al. synthesized CuS cathode with a reversible capacity around 390 $mAhg^{-1}$ after 100 cycles (0.5C,1.2−3.0 V).[14] Ren and co-workers have fabricated double-sandwich-like CuS@rGO as an anode showing a capacity of 412.5 mAh g^{-1} at 0.5 C (0.001−3.00 V).[29] Tao et al. synthesized CuS/graphene composite exhibiting a capacity of 296 mAh g^{-1} after 25 cycles (50 mA g^{-1}, 0.01−3.0 V).[28] To our knowledge, this large reversible capacity of CuS/rGO at 0.5C has not been witnessed in previous reports. The higher capacity and cycle stability can be attributed to the synergistic effect between CuS nanowires and rGO nanosheets as reported in the metal oxides/graphene composite and metal sulfide/graphene composite.[43,46,48,49] First, the unique structure contributes to the excellent electrochemical performance. On the one hand, the evenly distributed CuS nanowires could prevent rGO nanosheets from restacking, which can bring additional capacity from double-layer capacitance effect of rGO.[37] The capacitance effect was also suggested for enhanced Li-ion storage capacity in the graphene-based electrodes.[35,43] On the other hand, the introduction of rGO nanosheets can bind CuS nanowires and prevent these nanowires from aggregation, which can make full contact with the electrolyte and shorten the diffusion path of Li^+. Second, the conductivity of the composite would be dramatically enhanced due to the presence of rGO nanosheets. Therefore, the electronic transport length would be effectively shortened compared to pure CuS nanowires, leading to reduced particle−particle interface resistance.[50] Besides, the conductive graphene will help to relieve the rapid capacity fading. It is well-known the dissolution of Li_2S in the electrolyte will lead to a shuttle behavior and cause the rapid capacity fading. This is affected by the properties of anodes and electrolytes, and may be overcome by controlling and engineering the anode materials and electrolytes. Ether-based electrolytes, such as DOL/DME, were reported to show a better electrochemical performance than carbonate-based electrolytes.[16] However, in our work, the CuSNWs/rGO shows large reversible capacity and excellent stability when using carbonate-based EC/DEC/DMC as electrolytes. Apart from the influence of electrolyte, the graphene plays a vital role in improving electrochemical performance. The conductive graphene in the composite favors the electron transmission, such that most of the formed Li_2S upon reducing can be reoxidized, which attributed to the excellent electrochemical performance.[28,29] The porous and elastically strong nature of rGO nanosheets can also effectively

DOI: 10.1021/acsami.5b01285
ACS Appl. Mater. Interfaces 2015, 7, 15726−15734

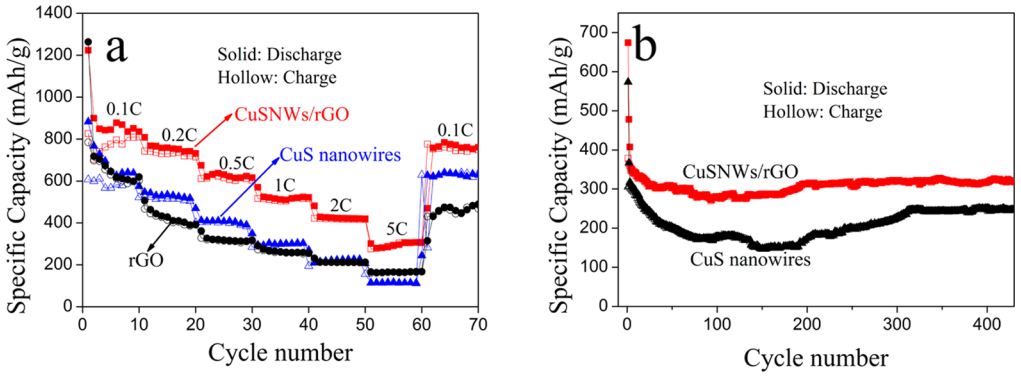

Figure 6. (a) Cycling performance of the CuSNWs/rGO nanocomposites electrode, CuS nanowires electrode and rGO electrode at various current densities. (b) Cycling performance of the CuSNWs/rGO nanocomposites electrode and CuS nanowireselectrode at 4C.

absorb polysulfide anions and confine their shuttle.[48] Hence, the issue of the capacity fading caused by dissolution of Li_2S is greatly alleviated, and the cycle stable is remarkably improved. As mentioned above, employing ether-based electrolytes is another promising way to improve the electrochemical performance and we should make a detailed study in future works.

Here, it can be found that the capacity of CuSNWs/rGO nanocomposites decreased to 530 mAh g^{-1} and then increased to 620 mAh g^{-1}, indicating a possible activation process of the electrode material.[18,29] This capacity recovery is related to the pseudocapacitive character of polymeric/gel films, which is similar to those observed in CoS_2/grapheme, mesoporous Co_9S_8 and transition metal oxides.[51−53] For example, in Jian Xie's report, the capacity of CoS_2/G reaches 900 mAh g^{-1}, far higher than that of the theoretical value of CoS_2/G. In the study by Yitai Qian's group, the specific capacity of Co_9S_8-650 gradually increases after first fading and then reaches 1400 mAh g^{-1} at the 100th cycle.

The high reversible capacity and excellent cycling behavior of the CuSNWs/rGO nanocomposites electrode are also exhibited in the rate capability. As shown in Figure 6a, at the maximum discharge rates studied, 5C (2.8A g^{-1}), the material delivers a capacity of 300 mAh g^{-1}, higher than 115, 165 mAh g^{-1} for CuS nanowires and rGO. Additionally, the extraordinary cycling stability of the CuSNWs/rGO electrode is exhibited at various current densities. When the charge/discharge current density changes from 5 to 0.1 C, the specific capacities of the composites return to 752 mAh g^{-1}, which do not ultimately change in the subsequent cycles, indicating extraordinarily high cycling stabilities. The excellent rate capability is also demonstrated in Figure 6b. At the current density of 4C, the capacity keeps stable and retains at 320 mAh g^{-1} even after 430 cycles, whereas the specific capacities of CuS nanowires is only 240 mAh g^{-1} and the stability is poor. The outstanding rate capability may be ascribed to two main aspects: (i) graphene acts as an elastic buffer and thereby accommodates volume expansion and shrinkage changes during the fast uptake and release of Li^+ at the high current; (ii) the superior conductivity of graphene enhances kinetics of the charge carrier transport.[44] The CuS has an electrical conductivity of about 10^{-3} S/cm, and rGO has an outstanding electrical conductivity of ∼10 S/cm.[54,55] From the TG analysis, the content of CuS in the CuSNWs/rGO nanocomposite is 82.40%, so we can approximately calculate the composite electrical conductivity is about 1.76 S/cm, which is significantly improved when rGO was introduced.

To obtain better understanding of the superior electrochemical performance of CuSNWs/rGO nanocomposites electrode compared to that of CuS nanowires electrode, electrochemical impedance spectroscopy (EIS) measurements were performed (inset in Figure 5c). The Nyquist plots are composed of a depressed semicircle in the high-to-medium frequency region and a sloping line in the low-frequency region. The depressed semicircle consists of two partly overlapped semicircles. The plots are fitted by an equivalent circuit.[25,37] As shown in the inset, the high-frequency semicircle region corresponds to SEI layer resistance and dielectric relaxation capacitance (R_f and CPE1), and the semicircle in the low-frequency region corresponds to the charge-transfer resistance R_{ct} and CPE2 of electrode/electrolyte interface. The inclined line is related to the lithium-diffusion process. The fitting results show that R_f and R_{ct} of CuS nanowires are 28.3 and 112.9 Ω, respectively. Although, the R_f and R_{ct} of CuSNWs/rGO composites are only 9.3 and 38.6 Ω, respectively. The result confirms that the incorporation of rGO nanosheets not only preserve the high conductivity of CuSNWs/rGO nanocomposites electrode but also significantly enhance rapid electron transfer during the electrochemical lithium insertion/extraction. Therefore, the CuSNWs/rGO nanocomposites electrode exhibits high reversible capacity, excellent cyclic stability and high-rate capability.

4. CONCLUSIONS

In a summary, CuSNWs/rGO nanocomposites were successfully synthesized by a facile one-pot method. The CuS nanowires are highly dispersed and anchored or wrapped in the rGO nanosheets. The composites exhibit excellent lithium-ion storage. Compared with the CuS electrode, it shows a significant higher capacity with a reversible capacity of 620 mAh g^{-1} at 0.5C after 100 cycles. Even at a high current density of 4C, the special capacity of CuSNWs/rGO nanocomposites electrode keeps stable and remains at 320 mAh g^{-1} after 500 cycles. The excellent lithium storage performance of the CuSNWs/rGO composites is mainly attributed to two aspects: (i) the CuSNWs/rGO nanocomposites can effectively accommodate large volume changes during the charge/discharge process; (ii) the presence of rGO nanosheets with superior electronic conductivity, supply 2D conducting network and absorb or trap the polysulfides generated during the conversion reaction of CuS, which improves the cycling stability of the electrode.

DOI: 10.1021/acsami.5b01285
ACS Appl. Mater. Interfaces 2015, 7, 15726−15734

■ ASSOCIATED CONTENT

Supporting Information

TG analysis of CuSNWs/rGO nanocomposites; SEM images of CuS nanowires; XPS analysis of CuSNW/rGO intermediate; charge and discharge curves for the CuS nanowires electrode; average cycling performance of the CuSNWs/rGO nanocomposites electrode at 0.5C; chemical equation of the possible reaction process of CuSNWs/rGO nanocompposite. The Supporting Information is available free of charge on the ACS Publications website at DOI: 10.1021/acsami.5b01285.

■ AUTHOR INFORMATION

Corresponding Authors

*K. Sun. E-mail: bitkeningsun@163.com. Fax: +86 10 68912185. Tel: +86 10 68918696.

*G. Liu. E-mail: gliu@lbl.gov. Fax: 00 510 4867207. Tel: 00510 4867303.

Notes

The authors declare no competing financial interest.

■ ACKNOWLEDGMENTS

The authors acknowledge the financial supports from the Creative Technology Project of Beijing Institute of Technology (No. 20131042005) and the support of Laboratory of Chemical Separation and Material Characterization, BIT.

■ REFERENCES

(1) Aricò, A. S.; Bruce, P.; Scrosati, B.; Tarascon, J. M.; Van, S. W. Nanostructured Materials for Advanced Energy Conversion and Storage Devices. *Nat. Mater.* **2005**, *4*, 366−377.

(2) Liu, C.; Li, F.; Ma, L.-P.; Cheng, H.-M. Advanced Materials for Energy Storage. *Adv. Mater.* **2010**, *22*, E28−E62.

(3) Yoo, H. D.; Markevich, E.; Salitra, G.; Sharon, D.; Aurbach, D. On the Challenge of Developing Advanced Technologies for Electrochemical Energy Storage and Conversion. *Mater. Today* **2014**, *17*, 110−121.

(4) Gao, M.-R.; Xu, Y.-F.; Jiang, J.; Yu, S.-H. Nanostructured Metal Chalcogenides: Synthesis, Modification, and Applications in Energy Conversion and Storage Devices. *Chem. Soc. Rev.* **2013**, *42*, 2986−3017.

(5) Balaya, P. Size Effects and Nanostructured Materials for Energy Applications. *Energy Environ. Sci.* **2008**, *1*, 645−654.

(6) Lai, C.-H.; Lu, M.-Y.; Chen, L.-J. Metal Sulfide Nanostructures: Synthesis, Properties and Applications in Energy Conversion and Storage. *J. Mater. Chem.* **2012**, *22*, 19−30.

(7) Wang, H.; Feng, H.; Li, J. Graphene and Graphene-Like Layered Transition Metal Dichalcogenides in Energy Conversion and Storage. *Small* **2014**, *10*, 2165−2181.

(8) Gao, M.-R.; Jiang, J.; Yu, S.-H. Solution-Based Synthesis and Design of Late Transition Metal Chalcogenide Materials for Oxygen Reduction Reaction (ORR). *Small* **2012**, *8*, 13−27.

(9) Ramasamy, K.; Malik, M. A.; Revaprasadu, N.; O'Brien, P. Routes to Nanostructured Inorganic Materials with Potential for Solar Energy Applications. *Chem. Mater.* **2013**, *25*, 3551−3569.

(10) Zhao, Y.; Burda, C. Development of Plasmonic Semiconductor Nanomaterials with Copper Chalcogenides for a Future with Sustainable Energy Materials. *Energy Environ. Sci.* **2012**, *5*, 5564−5576.

(11) Dennler, G.; Chmielowski, R.; Jacob, S.; Capet, F.; Roussel, P.; Zastrow, S.; Nielsch, K.; Opahle, I.; Madsen, G. K. H. Are Binary Copper Sulfides/Selenides Really New and Promising Thermoelectric Materials? *Adv. Energy Mater.* **2014**, *4*, 130581.

(12) Cai, R.; Chen, J.; Zhu, J.; Xu, C.; Zhang, W.; Zhang, C.; Shi, W.; Tan, H.; Yang, D.; Hng, H. H.; Lim, T. M.; Yan, Q. Synthesis of Cu_xS/Cu Nanotubes and Their Lithium Storage Properties. *J. Phys. Chem. C* **2012**, *116*, 12468−12474.

(13) Hsu, Y.-K.; Chen, Y.-C.; Lin, Y.-G. Synthesis of Copper Sulfide Nanowire Arrays for High-Performance Supercapacitors. *Electrochim. Acta* **2014**, *139*, 401−407.

(14) Wang, Y.; Zhang, X.; Chen, P.; Liao, H.; Cheng, S. In Situ Preparation of CuS Cathode with Unique Stability and High Rate Performance for Lithium Ion Batteries. *Electrochim. Acta* **2012**, *80*, 264−268.

(15) Feng, C.; Zhang, L.; Wang, Z.; Song, X.; Sun, K.; Wu, F.; Liu, G. Synthesis of Copper Sulfide Nanowire Bundles in a Mixed Solvent as a Cathode Material for Lithium-Ion Batteries. *J. Power Sources* **2014**, *269*, 550−555.

(16) Jache, B.; Mogwitz, B.; Klein, F.; Adelhelm, P. Copper Sulfides for Rechargeable Lithium Batteries: Linking Cycling Stability to Electrolyte Composition. *J. Power Sources* **2014**, *247*, 703−711.

(17) Han, F.; Li, W.-C.; Li, D.; Lu, A.-H. In Situ Electrochemical Generation of Mesostructured Cu_2S/C Composite for Enhanced Lithium Storage:Mechanism and Material Properties. *ChemElectroChem* **2014**, *1*, 733−740.

(18) Du, Y.; Yin, Z.; Zhu, J.; Huang, X.; Wu, X.-J.; Zeng, Z.; Yan, Q.; Zhang, H. A General Method for the Large-Scale Synthesis of Uniform Ultrathin Metal Sulphide Nanocrystals. *Nat. Commun.* **2012**, *3*, 1177.

(19) Zhang, B.; Gao, X.-W.; Wang, J.-Z.; Chou, S.-L.; Konstantinov, K.; Liu, H.-K. CuS Nanoflakes, Microspheres, Microflowers, and Nanowires: Synthesis and Lithium Storage Properties. *J. Nanosci. Nanotechnol.* **2013**, *13*, 1309−1316.

(20) Chen, Y.; Davoisne, C.; Tarascon, J.-M.; Guéry, C. Growth of Single-Crystal Copper Sulfide Thin Films via Electrodeposition in Ionic Liquid Media for Lithium Ion Batteries. *J. Mater. Chem.* **2012**, *22*, 5295−5299.

(21) Qiu, J.; Zhang, P.; Ling, M.; Li, S.; Liu, P.; Zhao, H.; Zhang, S. Photocatalytic Synthesis of TiO_2 and Reduced Graphene Oxide Nanocomposite for Lithium Ion Battery. *ACS Appl. Mater. Interfaces* **2012**, *4*, 3636−3642.

(22) Qiu, J.; Lai, C.; Wang, Y.; Li, S.; Zhang, S. Resilient Mesoporous TiO_2/Graphene Nanocomposite for High Rate Performance Lithium-Ion Batteries. *Chem. Eng. J.* **2014**, *256*, 247−254.

(23) Wang, X.; Li, G.; Hassan, F. M.; Li, M.; Feng, K.; Xiao, X.; Chen, Z. Building Sponge-Like Robust Architectures of CNT-Graphene-Si Composites with Enhanced Rate and Cycling Performance for Lithium-Ion Batteries. *J. Mater. Chem. A* **2015**, *3*, 3962−3967.

(24) Hassan, F. M.; Elsayed, A. R.; Chabot, V.; Batmaz, R.; Xiao, X.; Chen, Z. Subeutectic Growth of Single-Crystal Silicon Nanowires Grown on and Wrapped with Graphene Nanosheets: High-Performance Anode Material for Lithium-Ion Battery. *ACS Appl. Mater. Interfaces* **2014**, *6*, 13757−13764.

(25) Mahmood, N.; Zhang, C.; Jiang, J.; Liu, F.; Hou, Y. Multifunctional Co_3S_4/Graphene Composites for Lithium Ion Batteries and Oxygen Reduction Reaction. *Chem. - Eur. J.* **2013**, *19*, 5183−5190.

(26) Ji, L.; Rao, M.; Zheng, H.; Zhang, L.; Li, Y.; Duan, W.; Guo, J.; Cairns, E. J.; Zhang, Y. Graphene Oxide as a Sulfur Immobilizer in High Performance Lithium/Sulfur Cells. *J. Am. Chem. Soc.* **2011**, *133*, 18522−18525.

(27) Zhao, M.-Q.; Zhang, Q.; Huang, J.-Q.; Tian, G.-L.; Nie, J.-Q.; Peng, H.-J.; Wei, F. Unstacked Double-Layer Templated Graphene for High-Rate Lithium-Sulphur Batteries. *Nat. Commun.* **2014**, *5*, 3410.

(28) Tao, H.-C.; Yang, X.-L.; Zhang, L.-L.; Ni, S.-B. One-Pot Facile Synthesis of CuS/Graphene Composite as Anode Materials for Lithium Ion Batteries. *J. Phys. Chem. Solids* **2014**, *75*, 1205−1209.

(29) Ren, Y.; Wei, H.; Yang, B.; Wang, J.; Ding, J. Double-Sandwich-Like" CuS@Reduced Graphene Oxide as an Anode in Lithium Ion Batteries with Enhanced Electrochemical Performance. *Electrochim. Acta* **2014**, *145*, 193−200.

(30) Bai, J.; Jiang, X. A Facile One-Pot Synthesis of Copper Sulfide-Decorated Reduced Graphene Oxide Composites for Enhanced Detecting of H_2O_2 in Biological Environments. *Anal. Chem.* **2013**, *85*, 8095−8101.

(31) Zhang, Y.; Tian, J.; Li, H.; Wang, L.; Qin, X.; Asiri, A. M.; Al-Youbi, A. O.; Sun, X. Biomolecule-Assisted, Environmentally Friendly,

DOI: 10.1021/acsami.5b01285
ACS Appl. Mater. Interfaces 2015, 7, 15726−15734

One-Pot Synthesis of CuS/Reduced Graphene Oxide Nanocomposites with Enhanced Photocatalytic Performance. *Langmuir* **2012**, *28*, 12893−12900.
(32) Zhang, X.-J.; Wang, G.-S.; Wei, Y.-Z.; Guo, L.; Cao, M.-S. Polymer-Composite with High Dielectric Constant and Enhanced Absorption Properties Based on Graphene−CuS Nanocomposites and Polyvinylidene Fluoride. *J. Mater. Chem. A* **2013**, *1*, 12115−12122.
(33) Yeh, T.-F.; Syu, J.-M.; Cheng, C.; Chang, T.-H.; Teng, H. Graphite Oxide as a Photocatalyst for Hydrogen Production from Water. *Adv. Funct. Mater.* **2010**, *20*, 2255−2262.
(34) Wang, Y.; Zhang, L.; Jiu, H.; Li, N.; Sun, Y. Depositing of CuS Nanocrystals upon the Graphene Scaffold and Their Photocatalytic Activities. *Appl. Surf. Sci.* **2014**, *303*, 54−60.
(35) Gu, Y.; Xu, Y.; Wang, Y. Graphene-Wrapped CoS Nanoparticles for High-Capacity Lithium-Ion Storage. *ACS Appl. Mater. Interfaces* **2013**, *5*, 801−806.
(36) Sun, Y.; Hu, X.; Luo, W.; Xia, F.; Huang, Y. Reconstruction of Conformal Nanoscale MnO on Grapheneas a High-Capacity and Long-Life Anode Material for Lithium Ion Batteries. *Adv. Funct. Mater.* **2013**, *23*, 2436−2444.
(37) Pan, Q.; Xie, J.; Liu, S.; Cao, G.; Zhu, T.; Zhao, X. Facile One-Pot Synthesis of Ultrathin NiS Nanosheets Anchored on Graphene and the Improved Electrochemical Li-Storage Properties. *RSC Adv.* **2013**, *3*, 3899−3906.
(38) Larcher, D.; Sudant, G.; Patrice, R.; Tarascon, J. M. Some Insights on the Use of Polyols-Based Metal Alkoxides Powders as Precursors for Tailored Metal-Oxides Particles. *Chem. Mater.* **2003**, *15*, 3543−3551.
(39) Ma, X.-H.; Feng, X.-Y.; Song, C.; Zou, B.-K.; Ding, C.-X.; Yu, Y.; Chen, C.-H. Facile Synthesis of Flower-Like and Yarn-Like α-Fe_2O_3 Spherical Clusters as Anode Materials for Lithium-Ion Batteries. *Electrochim. Acta* **2013**, *93*, 131−136.
(40) Wankhede, M. E.; Haram, S. K. Synthesis and Characterization of Cd-DMSO Complex Capped CdS Nanoparticles. *Chem. Mater.* **2003**, *15*, 1296−1301.
(41) Stone, J. A.; Su, T.; Vukomanovic, D. A Collisionally Activated Dissociation (CAD) and Computational Investigation of Doubly and Singly Charged DMSO Complexes of Cu^{2+}. *Can. J. Chem.* **2005**, *83*, 1921−1935.
(42) Cotton, F. A.; Francis, R.; Horrocks, W. D. Sulfoxides as Ligands. II. The Infrared Spectra of Some Dimethyl Sulfoxide Complexes. *J. Phys. Chem.* **1960**, *64*, 1534−1536.
(43) Guo, P.; Song, H.; Chen, X. Electrochemical Performance of Graphene Nanosheets as Anode Material for Lithium-Ion Batteries. *Electrochem. Commun.* **2009**, *11*, 1320−1324.
(44) Wang, Z.; Chen, T.; Chen, W.; Chang, K.; Ma, L.; Huang, G.; Chen, D.; Lee, J. Y. CTAB-Assisted Synthesis of Single-Layer MoS_2−Graphene Composites as Anode Materials of Li-Ion Batteries. *J. Mater. Chem. A* **2013**, *1*, 2202−2210.
(45) Xu, C.; Zeng, Y.; Rui, X.; Xiao, N.; Zhu, J.; Zhang, W.; Chen, J.; Liu, W.; Tan, H.; Hng, H. H.; Yan, Q. Controlled Soft-Template Synthesis of Ultrathin C@FeS Nanosheets with High-Li-Storage Performance. *ACS Nano* **2012**, *6*, 4713−4721.
(46) Huang, X.-L.; Wang, R.-Z.; Xu, D.; Wang, Z.-L.; Wang, H.-G.; Xu, J.-J.; Wu, Z.; Liu, Q.-C.; Zhang, Y.; Zhang, X.-B. Homogeneous CoO on Graphene for Binder-Free and Ultralong-Life Lithium Ion Batteries. *Adv. Funct. Mater.* **2013**, *23*, 4345−4353.
(47) Cheng, J.; Pan, Y.; Zhu, J.; Li, Z.; Pan, J.; Ma, Z. Hybrid Network CuS Monolith Cathode Materials Synthesized via Facile in Situ Melt-Diffusion for Li-Ion Batteries. *J. Power Sources* **2014**, *257*, 192−197.
(48) Mahmood, N.; Zhang, C.; Hou, Y. Nickel Sulfide/Nitrogen-Doped Graphene Composites: Phase-Controlled Synthesis and High Performance Anode Materials for Lithium Ion Batteries. *Small* **2013**, *9*, 1321−1328.
(49) Zhou, X.; Zhang, J.; Su, Q.; Shi, J.; Liu, Y.; Du, G. Nanoleaf-on-Sheet CuO/Graphene Composites: Microwave-Assisted Assemble and Excellent Electrochemical Performances for Lithiumion Batteries. *Electrochim. Acta* **2014**, *125*, 615−621.
(50) Nethravathi, C.; Rajamathi, C. R.; Rajamathi, M.; Wang, X.; Gautam, U. K.; Golberg, D.; Bando, Y. Cobalt Hydroxide/Oxide Hexagonal Ring-Graphene Hybrids through Chemical Etching of Metal Hydroxide Platelets by Graphene Oxide: Energy Storage Applications. *ACS Nano* **2014**, *8*, 2755−2765.
(51) Zhou, Y.; Yan, D.; Xu, H.; Feng, J.; Jiang, J.; Yue, J.; Yang, J.; Qian, Y. Hollow Nanospheres of Mesoporous Co_9S_8 as a High-Capacity and Long-Life Anode for Advanced Lithium Ion Batteries. *Nano Energy* **2015**, *12*, 528−537.
(52) Xie, J.; Liu, S.; Cao, G.; Zhu, T.; Zhao, X. Self-Assembly of CoS_2/Grapheme Nanoarchitecture by a Facile One-Pot Route and Its Improved Electrochemical Li-Storage Properties. *Nano Energy* **2013**, *2*, 49−56.
(53) Laruelle, S.; Grugeon, S.; Poizot, P.; Dollé, M.; Dupont, L.; Tarascon, J. M. On the Origin of the Extra Electrochemical Capacity Displayed by MO/Li Cells at Low Potential Batteries and Energy Conversion. *J. Electrochem. Soc.* **2002**, *149*, A627−A634.
(54) Marinho, B.; Ghislandi, M.; Tkalya, E.; Koning, C. E.; de With, G. Electrical Conductivity of Compacts of Graphene, Multi-Wall Carbon Nanotubes, Carbon Black, and Graphite Powder. *Powder Technol.* **2012**, *221*, 351−358.
(55) Ding, J. N.; Fan, Y.; Zhao, C. X.; Liu, Y. B.; Yu, C. T.; Yuan, N. Y. Electrical Conductivity of Waterborne Polyurethane/Graphene Composites Prepared by Solution Mixing. *J. Compos. Mater.* **2012**, *46*, 747−752.

DOI: 10.1021/acsami.5b01285
ACS Appl. Mater. Interfaces 2015, 7, 15726−15734